

Phylogenetics of *Planipapillus*, Lawn-Headed Onychophorans of the Australian Alps, Based on Nuclear and Mitochondrial Gene Sequences

Matthew V. Rockman,^{*,1} David M. Rowell,^{*} and Noel N. Tait[†]

^{*}Department of Botany and Zoology, Australian National University, Canberra, ACT 0200, Australia; and

[†]Department of Biological Science, Macquarie University, Sydney, NSW 2109, Australia

Received January 29, 2001; revised March 28, 2001

We addressed phylogenetic relationships among species of *Planipapillus*, a clade of oviparous onychophorans from southeastern mainland Australia, to create a framework for understanding the evolution of the modified male head papillae used in mating in this clade. We sequenced fragments of two mitochondrial genes, COI and 12S rRNA, and a nuclear intron from the *fushi tarazu* gene, for individuals from 14 putative species of *Planipapillus* and six outgroups. We analyzed these data under both parsimony and likelihood criteria, incorporating heterogeneous parameter fitting guided by likelihood ratio tests. These analyses result in strong, congruent support for many clades. We infer multiple independent origins of spikes in *Planipapillus* male head structures. © 2001 Academic Press

INTRODUCTION

Onychophorans are soft-bodied terrestrial invertebrates with lobopodial limbs arranged segmentally along their trunks, each limb terminating in a pair of claws. Commonly called peripatus or velvet worms, they are widely distributed in southern hemisphere temperate regions and in the tropics. Onychophorans are vulnerable to desiccation and hence largely confined to moist, humid microhabitats, including leaf litter and the interior of decomposing logs, where they are predators on small invertebrates.

Onychophorans are often considered evolutionarily static “living fossils” (Ghiselin, 1984) with affinities to Cambrian forms (Ramskold and Junyuan, 1998), relatively unchanged in the more than 300 million years since the Carboniferous (Thompson and Jones, 1980; Heyler and Poplin, 1988). Recent studies, however, have revealed an extraordinary diversity among extant onychophorans at several levels. Allozyme and nucleo-

tide sequence studies have exposed a wealth of variation indicative of extensive and ancient radiations of onychophorans in Australia and New Zealand (Briscoe and Tait, 1995; Tait and Briscoe, 1995; Tait *et al.*, 1995; Gleeson *et al.*, 1998; Trewick, 1998, 1999, 2000; Sunnucks *et al.*, 2000b). Rowell *et al.* (1995) demonstrated a wide range of distinct karyotypes, with variation evident even among sister species (Reid *et al.*, 1995). Finally, detailed studies of morphology have revealed that the molecular and karyotypic divergences are paralleled by morphological differentiation, culminating in the description of 64 species within Australia (Reid, 1996, 2000). One surprising result of these morphological studies was the identification of a suite of modifications of the integument of the head of males, including patches of modified dermal papillae and eversible pits which, in some species, contain hardened tusks, spikes, or stylets (Tait and Briscoe, 1990; Reid, 1996, 2000). The description of mating behavior in *Planipapillus annae* and *Florellicept stutchburyae* indicate that these head structures function in the transfer of a spermatophore to the posterior genital opening of females (Reid, 2000; Tait and Norman, 2001).

Given the new broad perspectives on onychophoran diversity, we have focused our attention on a single clade of closely related species belonging to *Planipapillus* Reid, 1996 to provide a better characterization of the features underlying the evolution of the Australian onychophoran fauna. An understanding of the population- and species-level diversity is also critical for the conservation of these potentially threatened but poorly known animals (New, 1995; Trewick, 1999). *Planipapillus*, a clade confined to the southeastern corner of mainland Australia, is of particular interest as preliminary studies indicated distinctive patterns of morphological and chromosomal variation which, when analyzed together, may permit the development of an inclusive model for the origin and radiation of this group. *Planipapillus* females are oviparous and possess ovipositors, features found only in some lineages

¹To whom correspondence should be addressed at present address: Department of Biology, Duke University, Box 90338, Durham, NC 27708. E-mail: mrockman@duke.edu.

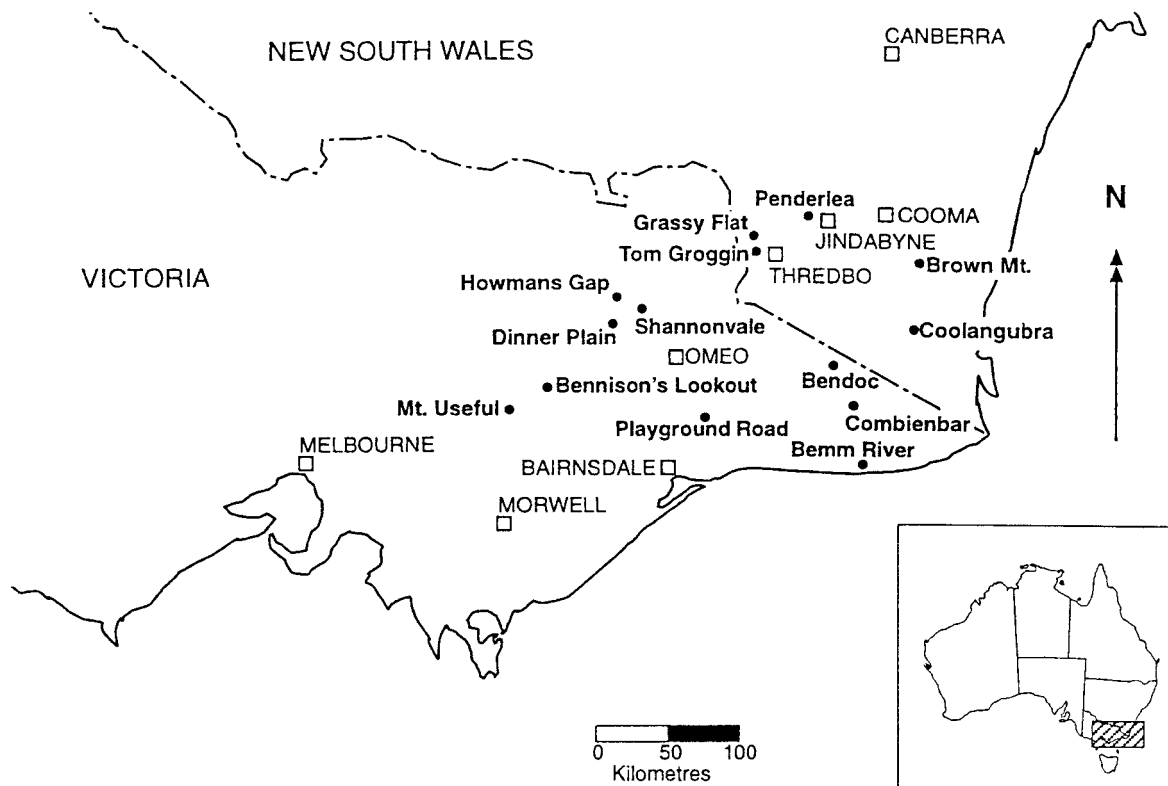


FIG. 1. Locality map for *Planipapillus* collection sites.

confined to Australia and New Zealand (Reid, 1996). The remaining species of Australian onychophorans are ovoviviparous with yolky eggs and give birth to active young. The evolutionary relationships among oviparous and ovoviviparous species are unresolved (Reid, 1996; Gleeson *et al.*, 1998), although the phylogeny may be interpreted as implying that ovoviviparity is the ancestral state in the Onychophora, with derived oviparity having arisen on a number of occasions (Reid, 1996).

Planipapillus males have a patch of reduced papillae on the dorsal surface of their heads, just posterior to the eyes. In some species, these patches are elaborated by the presence of spines on the posterior margin (Tait and Briscoe, 1990; Reid, 1996). The relationships among *Planipapillus* and other Australian genera possessing head structures are uncertain. Reid (1996) considered eversible head structures to be homologous to modified papillae anterior to the eyes; such modified papillae are absent in *Planipapillus*. Thus, Reid's analysis treated modified papillae posterior to the eyes (as in *Planipapillus*) and anterior to the eyes (as in some other species and including eversible structures) as nonhomologous features. One of our goals is to place these head structures in a phylogenetic context as a first step to understanding their homologies and evolutionary histories.

Twelve species have been described within *Planipapillus* (Reid 1996, 2000). Whereas *Planipapillus* appears to be monophyletic, a phylogenetic analysis based on morphological characters did not resolve relationships within the clade (Reid, 2000). This may be due to species diagnoses based largely on the male modified head papillae, which by themselves are insufficiently informative. Here we use an independent data set of nucleotide sequences to formulate hypotheses about the evolution of the head structure within *Planipapillus*. These analyses also include species displaying a variety of head structure types and female reproductive strategies as outgroups.

MATERIALS AND METHODS

Specimens

Specimens of *Planipapillus* were hand-collected from 14 localities in New South Wales and Victoria, Australia (Fig. 1, Table 1). All specimens were collected from within or under rotting logs. Specimens from 5 of the populations are referable to described *Planipapillus* species on the basis of head structure morphology and locality as in Reid (1996, 2000). Others did not conform to a species diagnosis or their identity is uncertain as they were collected from a locality previously unsampled by Reid. All of these undiagnosed popula-

TABLE 1
Collection Data

Species	Locality	Coordinates	Modified papillae
<i>P. biacinaces</i>	Howman Gap, Vic	36° 51'S 147° 15'E	Class 4
<i>P. cyclus</i>	Combienbar, Vic	37° 28'S 148° 55'E	Class 3
<i>P. impacris</i>	Coolangubra, NSW	37° 01'S 149° 23'E	Class 3
<i>P. mundus</i>	Penderlea, NSW	36° 26'S 148° 30'E	Class 1
<i>P. taylori</i>	Brown Mt., NSW	36° 37'S 149° 21'E	Class 2
<i>P. sp. 1</i>	Grassy Flat, NSW	36° 29'S 148° 08'E	Class 1
<i>P. sp. 2</i>	Tom Groggin, NSW	36° 33'S 148° 08'E	Class 1
<i>P. sp. 3</i>	Playground Rd, Vic	37° 35'S 147° 53'E	Class 1
<i>P. sp. 4</i>	Bennison's Lookout, Vic	37° 30'S 146° 41'E	Class 1
<i>P. sp. 5</i>	Mt. Useful, Vic	37° 43'S 146° 32'E	Class 6
<i>P. sp. 6</i>	Shannonvale, Vic	36° 55'S 147° 25'E	Class 5
<i>P. sp. 7</i>	Bendoc, Vic	37° 09'S 148° 53'E	Class 3
<i>P. sp. 8</i>	Dinner Plain, NSW	37° 01'S 147° 15'E	Class 4
<i>P. sp. 9</i>	Bemm River, Vic	37° 40'S 148° 54'E	Unknown

tions differed chromosomally from otherwise morphologically similar species (D. M. Rowell *et al.*, in press). These populations are here designated by numerals following Rowell *et al.* (in press) as shown in Table 1 and by locality names.

Reid (1996) described *P. bulgensis* from Tarra-Bulga National Park, but in approximately 6 person-days of searching we were unable to collect any *Planipapillus* at this site, and we were thus unable to include this species in our sequencing efforts. Additionally, our collection from *Planipapillus* sp. 9, Bemm River, included no males, and so we were unable to characterize the male head structure of this population.

The techniques of DNA preparation and scanning electron microscopy (SEM) are destructive, but wherever possible voucher specimens of both sexes were lodged at the Australian Museum in Sydney.

Phylogenetic analysis of morphological (Reid, 1996) and molecular (Gleeson *et al.*, 1998) data have been unable to identify firmly the sister clade to *Planipapillus*. In addition, we believe that the sequence labeled *Planipapillus* in the study of Gleeson *et al.* (1998) may have been misidentified. Consequently, the closest outgroup to *Planipapillus* is unknown. Accordingly, we selected six outgroup taxa for our phylogenetic analyses: two taxa, *Baeothele saukros* and *Ooperipatus* sp., Bendoc, Victoria, are oviparous and are sexually dimorphic, with males possessing modified dorsal head papillae anterior to the eyes; three taxa, *Cephalofovea tomahmontis*, *Phalloecephale tallagandensis*, and *Ruhbergia bifalcata*, are ovoviviparous and sexually dimorphic, with males possessing eversible head structures; and *Euperipatoides rowelli*, an ovoviviparous taxon with no male head modification, is a more distant outgroup according to Reid (1996). Specimens of outgroup taxa were collected as above.

Scanning Electron Microscopy

Specimens were prepared for SEM according to Tait and Briscoe (1990).

DNA Extractions, Primers, PCR, and Sequencing

Whole genomic DNA was extracted from body segments after removal of the gut. Tissue was repeatedly soaked in TE9 buffer (Shiozawa *et al.*, 1992) for several hours to leach pigments, which may act as PCR inhibitors (Sunnucks and Wilson, 1999). Tissues were then homogenized in 250 μ l TE9 and incubated overnight at 65°C after the addition of 30 μ l 20% SDS and 5 μ l 10 mg/ml proteinase K. Protein was precipitated with ammonium acetate, and DNA was precipitated from the supernatant with ethanol. The DNA was washed in 70% ethanol and resuspended in 25 μ l of TE buffer. The DNA was further purified by incubation at 65°C with 10% chelex prior to PCR.

DNA sequences of subunit 1 of the mitochondrial cytochrome *c* oxidase gene (COI) were amplified with the bugnet kit primers mtD6 and mtD9, described by Simon *et al.* (1994) as C1-J-1718 and C1-N-2191. Sequences of the mitochondrial small subunit (12S) rRNA gene were amplified with the bugnet kit primers mtD35 and mtD36, SR-J-14233 and SR-N-14588 of Simon *et al.* (1994). Sequences of intronic DNA from the nuclear gene *fushi tarazu* (*ftz*) were amplified with primers designed with the aid of PRIMER version 0.5 (Lincoln *et al.*, 1991) based on the onychophoran (*Acanthokara kaputensis*) sequence from Grenier *et al.* (1997) and additional sequences from GenBank for a centipede (*Ethmostigmus rubripes*, AF010177), fly (*Drosophila melanogaster*, X00854), and beetle (*Tribolium castaneum*, U14732). The primer pair *ftz*118 and *ftz*rev were used in most cases; where these failed the partially overlapping

upstream primer ftz109 was substituted for ftz118. Sequences are given below, with Y=C/T and W=A/T:

ftz118 (22mer): 5'-CCTTGGATGAGATCCTATACWG-3'
 ftz109 (18mer): 5'-CCTCTTATCCTTGGATG-3'
 ftzrev (18mer): 5'-GCCTCGTTCYTTTGGYC-3'

Most reactions were carried out in 20–25 μ l, and typical reaction conditions included 1 \times PCR buffer, 2.5 mM MgCl₂, 0.5 μ M dNTPs, 0.2 μ M primers, and 1 unit of *Taq*. PCR mixes were irradiated with UV prior to the addition of *Taq* polymerase and template DNA to destroy possible contaminants. Negative controls were checked for all reactions, and only products from clean runs were sequenced. The typical thermal cycling program involved 2 min at 94°C for preliminary denaturation, then cycles of 30 s at 94°C for the denaturation step, then an annealing step of 40 s (at 60°C for the first two cycles, then 55°CX2 cycles, 50°CX4, 45°CX4, and finally 40°CX28), and each cycle concluded with 1 min at 72°C for extension.

PCR products were isolated on 1% agarose gels and purified with the BresaClean method. Products were sequenced in both directions with BigDye cycle sequencing and an ABI 377 automated sequencer. The gels were read with Sequencher software (Gene Codes Corp.). Sequences with primers excised have been deposited in GenBank under Accession Nos. AF337980–AF338037.

For the COI data, several individuals were sequenced from many localities. Bases scored for phylogenetic analysis as variable in this data set are polymorphic; i.e., they differed among the individuals. In the other data sets, one individual was sequenced for most localities and bases scored as variable were ambiguous on the sequencing gels.

COI sequences for *Euperipatoides rowelli* (U62425), *Phalloecephale tallagandensis* (U62407), and *Cephalofovea tomahmontis* (U62405) are from Gleeson *et al.* (1998).

Sequence Analysis

Sequences were aligned with Clustal X (Thompson *et al.*, 1997), considering a range of gap penalties to identify ambiguous regions. The final alignment is available in NEXUS format at <http://www.duke.edu/~mrockman/Planipapillus.html>. Paup* (Swofford, 1998) was used for phylogenetic analyses.

Tree searches under the maximum-parsimony criterion (MP) entailed 100 replicates of random sequence addition with tree bisection and reconnection (TBR) branch swapping. To determine MP support (decay) indices (Bremer, 1988), length criteria were relaxed stepwise and strict consensus of the resulting tree sets were calculated. MP bootstraps (Felsenstein, 1985) included 1000 bootstrap samples and searches involving 10 replicates of random sequence addition and TBR branch swapping.

Model fit for maximum-likelihood (ML) analysis was tested with likelihood ratio tests (LRTs) on nested models. We compared models with equal and unequal nucleotide frequencies, one, two, three, or six substitution types, equal rates among sites or gamma-distributed rates, and all sites variable or a proportion of sites invariable. LRTs allow nonarbitrary selection of a likelihood model (Goldman, 1993; Yang *et al.*, 1995; Huelsenbeck and Crandall, 1997), and use of the best-fit model determined by LRTs has been shown empirically to improve phylogenetic accuracy (Cunningham *et al.*, 1998). LRT statistics were tested against modified χ^2 distributions (Goldman and Whelan, 2000). Gamma distributions were approximated by four-category discrete distributions.

Searches under the maximum-likelihood criterion started with model parameters fixed to the values estimated from the Jukes-Cantor (JC) ML topology (Jukes and Canter, 1969). The highest-likelihood topology with these parameters, identified by a heuristic search with 10 replicates of random sequence addition and TBR branch swapping, was then used to estimate new values for the model parameters. Additional rounds of tree searching and parameter reestimation followed until no increases in likelihood scores were found. ML bootstraps included 100 bootstrap samples, each with 10 replicates of random sequence addition and TBR branch swapping. For each bootstrap sample, likelihood model and parameter values were fixed to the model and final parameter values identified in the original analysis.

To test nucleotide frequency stationarity, we calculated a χ^2 statistic for each data set as implemented in PAUP*. Because the sequences are not phylogenetically independent, the test statistic is not χ^2 distributed and the null distribution must be generated by simulation. After excluding gapped sites, we estimated branch lengths and other model parameters on the JC test tree for each data set using the best-fit ML model for the data. These parameters were then used to simulate 100 data sets in PAML (Yang, 2000). The distributions of χ^2 statistics for these simulated data sets were then used as the null distributions. Because the best-fit model for the COI data includes a proportion of invariable sites, which may lower χ^2 values by inflating the expected values, we first excluded the ML-estimated fraction of constant sites, in proportion to the nucleotide frequencies of the constant sites.

The three sequence data sets were tested for homogeneity (combinability) with the MP partition homogeneity test (Farris *et al.*, 1995), as implemented in Paup*, with MP-informative sites only and 100 replicates. Concatenated sequences were analyzed under the parsimony and likelihood criteria with a homogeneous model (i.e., assuming that the processes of sequence evolution were homogeneous among the partitions). In addition, the concatenated sequences were

analyzed under the likelihood criterion with a heterogeneous model, i.e., with different parameter estimates, including branch lengths, assigned to each of the three gene sequence partitions (Yang, 1996). Process homogeneity was tested in the ML framework by means of LRTs. Incongruence between gene trees can be due either to different underlying topologies (due to lineage sorting, for example) or to different sequence evolution dynamics on a single topology. ML with the heterogeneous process model accommodates the latter source of incongruence.

Topologies were compared with the nonparametric multiple comparisons approach of Shimodaira and Hasegawa (1999; see also Goldman *et al.*, 2000; Buckley *et al.*, 2001). This modification of the conventional testing approach of Kishino and Hasegawa (1989) is necessitated by the use of *a posteriori* topologies chosen on the basis of their likelihood and parsimony scores. One hundred nonparametric bootstrap replicates of the data were generated in the Seqboot module of Phylip (Felsenstein, 2000). A pool of 60 candidate trees, including all trees favored under the parsimony or likelihood criterion in any analysis of any partition of the data, was used as the test topology set. Likelihood Shimodaira–Hasegawa tests (LSH) employed full parameter optimization on every topology with each bootstrapped data set (test *posNPFcd* of Goldman *et al.*, 2000). Parsimony SH tests (PSH) were implemented as described by Shimodaira and Hasegawa (1999), but substituting tree lengths for negative log likelihoods. SH tests are very conservative and have low power to reject topologies, but they lack the inherent bias of *a posteriori* applications of the Kishino–Hasegawa test. In the present case, the inappropriate but usual application of the KH test gives very different results from the SH test, rejecting many more trees.

RESULTS

Head Structures

We recognize six general classes of head structures in *Planipapillus*. The first class (Figs. 2A and 2B) features an ovoid patch of reduced papillae on the dorsum of the head as described for *P. mundus* by Reid (1996) and here collected from Penderlea, a site included in the locality list for this species. It is from this feature that *Planipapillus* derives its common name, the lawn-headed peripatus. Specimens of males of *Planipapillus* sp. 1 (Grassy Flat), *Planipapillus* sp. 2 (Tom Groggin), *Planipapillus* sp. 3 (Playground Road), and *Planipapillus* sp. 4 (Bennison's Lookout) also display this class of head structure, as do *P. annae*, *P. berti*, *P. bulgensis*, *P. gracilis*, *P. tectus*, and *P. vittatus* (Reid, 2000).

The second class of head structure (Fig. 2C) consists of four forward-pointing sclerotized spikes of equal length in an ovoid patch on the dorsum of the head as

described for *P. taylori* by Reid (1996) and here collected from Brown Mt., a site close to the type locality of Bombala River.

The third class (Fig. 2D), consisting of four sclerotized spikes with the outer pair longer than the inner pair, characterizes *P. impacris*, described by Reid (1996) and here collected from the type locality of Coolangubra, and *P. cycclus*, described by Reid (2000) and here collected from the type locality of Combienbar. *P. sp. 7* (Bendoc) also displays this characteristic.

The fourth class (Fig. 2E) consists of two small sclerotized spikes in an ovoid patch on the dorsum of the head as for *P. biacinaces* as described by Reid (1996) and here collected from the type locality of Howman's Gap. *P. sp. 8* (Dinner Plain) also displays this class of male head papillae, as does *P. biacinooides* (Reid, 2000).

The fifth class (Fig. 2F) consists of two longitudinal rows of tusk-like sclerotized spikes with a row of smaller tusks on each side of each row of larger tusks. This head structure has not previously been reported and characterizes male specimens of *P. sp. 6* (Shannonvale).

P. sp. 5 (Mt. Useful) is unique in that males have unmodified head papillae (class 6).

ftz Intron Sequences

Except for three small regions of length variation, the *ftz* intron sequences are highly conserved. The intron ranges in length from 313 to 336 bp among the 20 taxa represented in the alignment. The final alignment includes 377 sites, 36 of which are in the three regions of ambiguous positional homologies and the last 12 of which are protein-coding sites from the gene's homeo-domain-containing exon. Of the 341 alignable positions of the *ftz* sequences, 31 are variable and 11 parsimony informative. In addition, the alignment includes six MP-informative indels, which were coded as binary characters, and three length-variable regions of ambiguous alignment, which were coded as unordered characters with 5, 10 and 12 states for MP analysis. Within *Planipapillus*, 12 nucleotide sites are variable; 6 nucleotide sites and six of the other characters are MP informative within the ingroup.

The average base frequencies of the sequenced region are highly A+T biased (Table 2) and there is no significant heterogeneity among sequences ($P > 0.38$).

The 12 shortest MP trees for the 20 taxa were each 70 steps (CI on informative characters = 0.8776, RI = 0.8723). The strict consensus tree (Fig. 3a) supports *Planipapillus* monophyly but roots the clade at a basal polytomy. Analyses of the nucleotide and indel partitions separately indicate that they support similar sets of relationships; numbers of characters in these data sets are too small for any statistical test of homogeneity to be useful.

Whereas parsimony analysis makes use only of the informative sites, the amount of data analyzed can be

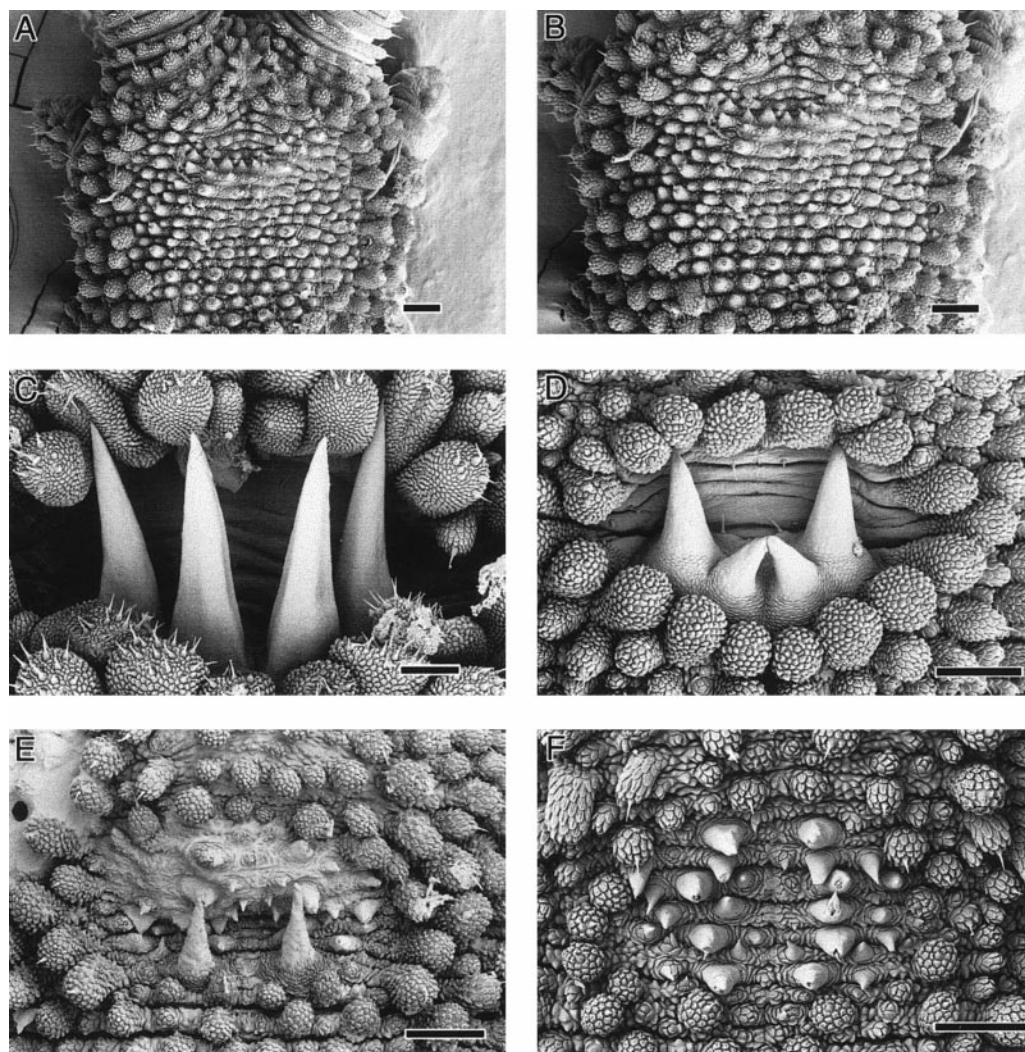


FIG. 2. Scanning electron micrographs of *Planipapillus* head structures. Scale bar, 100 μm . (A) Dorsal surface of the head of *P. mundus* to show the position of the modified papillae posterior to eyes. The bases of the antennae are at the top of the image and the lateral appendages are the slime papillae. (B) Higher power of class 1 head structure of *P. mundus* displaying ovoid patch of reduced papillae without sclerotized spikes. (C) Class 2 head structure of *P. taylora* displaying four equal-sized sclerotized spikes. (D) Class 3 head structure of *P. impacris* displaying four unequal-sized spikes. (E) Class 4 head structure of *P. biacinaces* displaying two sclerotized spikes. (F) Class 5 head structure of *P. sp. 6* (Shannonvale) displaying rows of large and smaller spikes.

expanded by maximum-likelihood analysis, which takes both the constant and the uninformative sites into account in calculating tree likelihoods. Nested LRTs indicated that model fit was significantly improved by the rejection of the hypothesis of equal frequencies of each nucleotide ($P < 0.00001$). Other generalizations on the JC model did not significantly improve model fit (equal rates for transitions and transversions, $P = 0.70$; equal rates among sites, $P > 0.9$; no invariable sites, $P = 0.24$). Maximum-likelihood analysis under the LRT-favored F81 model (Felsenstein, 1981), incorporating ML-estimated equilibrium base frequencies ($\hat{\pi}_A = 0.31941$, $\hat{\pi}_C = 0.11126$, $\hat{\pi}_G = 0.13237$), yields more than 25,000 trees, differing only in the placement of zero-length branches. When

these branches are collapsed, there is a single tree ($-\ln L = 664.92596$; Fig. 3b), consistent with those derived under parsimony but less resolved due to the exclusion of the indel characters from this analysis.

COI Sequences

The COI sequences include 473 sites. COI was sequenced from multiple animals from several localities to gauge polymorphism, which was detected in two of the five populations examined, with single nucleotide transitions in each case (Table 3). These levels of nucleotide diversity are low relative to the differences among populations; the most closely related populations differ by five [*P. sp. 5* (Mount Useful) and *P. sp. 4* (Bennison's Lookout)] and eight [*P. sp. 2* (Tom Groggin)

TABLE 2
Summary Statistics for Sequence Data

	<i>ftz</i> Intron	COI	1st	2nd	3rd	12S
Aligned Sites	341	473	158	157	158	338
Ingroup						
%A	31.1	27.7	25.4	14.7	42.9	39.0
%C	9.9	15.1	15.6	27.4	2.5	7.1
%G	11.9	16.0	25.8	16.6	5.6	10.4
%T	47.0	41.2	33.2	41.4	49.0	43.4
Variable	12	96	5	0	91	45
MP informative	6 (12) ^a	70	3	0	67	19
All taxa						
%A	31.3	28.4	25.5	14.7	44.9	39.2
%C	10.0	15.0	15.2	27.6	2.3	7.0
%G	12.0	15.8	25.9	16.5	5.1	10.6
%T	46.7	40.8	33.4	41.3	47.7	43.2
Variable	31	145	20	4	121	113
MP informative	11 (20) ^a	101	9	1	91	65

^a The *ftz* intron alignment includes 371 sites, 341 of which are confidently alignable. The remaining sites were recoded as indels and included in parsimony analysis as 9 additional characters, for a total of 12 characters informative within the ingroup and 20 overall.

and *P. sp. 1* (Grassy Flat)] substitutions in the COI sequences. The diversity is also exceptionally low compared to that of *Euperipatoides rowelli*. Sunnucks *et al.* (2000b) found up to eight COI haplotypes from the *E. rowelli* collected in a single log, with nucleotide divergence of up to 12.7% among the haplotypes. Gleeson *et al.* (1998) found that high levels of intraspecific COI variation also characterize *Ooperipatellus insignis* (11%) and *Peripatoides novaezealandiae* (7%). These taxa most likely represent species complexes, as has proved true for many widespread onychophoran taxa (Trewick, 1998, 1999, 2000; Reid, 1996; Reid *et al.*, 1995; Briscoe and Tait, 1995; Sunnucks and Wilson, 1999).

Ingroup variation is concentrated in the third position of codons; 5, 0, and 91 sites are variable at the first, second, and third positions, respectively (Table 2). Even in third positions, variation is limited; 42% of third positions are invariant, and 30% are invariant even when only fourfold degenerate sites are considered. Uncorrected pairwise ("p") distances range from 0.011 to 0.116. At the low end, these distances are comparable to typical invertebrate sibling species distances of around 3% (Trewick, 1999). At the same time, the total divergence of *Planipapillus* COI is less than the COI divergence characterizing *E. rowelli* individuals from a single log (Sunnucks *et al.*, 2000b).

At the amino acid level, the ingroup sequences are invariant except for a single autapomorphic serine in *P. taylori*; the homologous residue is glycine in the other *Planipapillus* sequences and is highly variable among other Australasian onychophorans (Gleeson *et al.*, 1998).

When all 20 taxa are considered, there are 145 variable positions, 101 of which are MP informative (Table 2). Nucleotide frequencies are strongly A+T biased, particularly at third positions (Table 2). Overall frequencies are homogeneous among the sequences ($P > 0.07$).

Parsimony analysis results in four shortest trees, each 366 steps (CI = 0.5016; RI = 0.5911). The strict consensus tree, with decay indices and bootstrap proportions, is shown in Fig. 4a. *Planipapillus* monophyly is strongly supported, although the relationships among the outgroups are unresolved. The ingroup is rooted on the branch separating *P. mundus* from the remaining taxa. The remaining ingroup taxa are split into two major clades, one including the five taxa from the eastern edge of the *Planipapillus* distribution and another clade including the taxa from western *Planipapillus* localities, centered on the main range of the Australian Alps.

For ML analysis, nested LRTs indicated that model fit is significantly improved with incorporation of several parameters. The hypotheses of equal base frequencies, equal transition and transversion rates, equal rates among transition and transversion types, equal rates among sites, and no invariable sites were all strongly rejected ($P < 0.005$). The six-substitution-type general time reversible (GTR) model does not improve fit significantly over three-substitution-type models, of which Kimura's (1981) model gives the highest likelihood. We therefore used a version of Kimura's model, which includes two transversion types and one transition type, modified to incorporate unequal nucleotide frequencies, gamma-distributed among-site rate

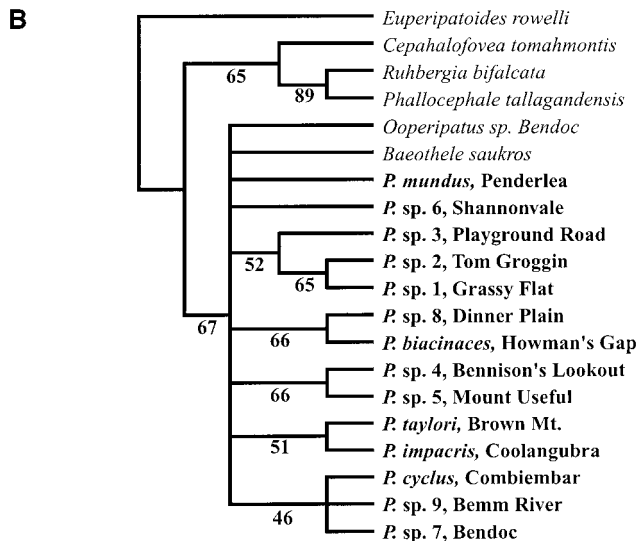
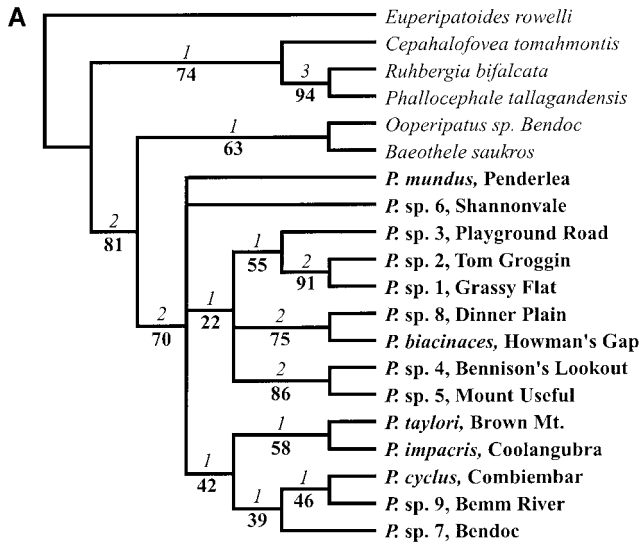


FIG. 3. Phylogenetic trees of *ftz* intron sequences, with *Planipapillus* species in boldface. (a) Strict consensus of 12 most parsimonious trees, showing decay support values above the branches and bootstrap percentages below. (b) ML tree, zero-length branches collapsed, showing bootstrap percentages.

variation, and a proportion of invariable sites (K3STf+ Γ +I). Note that Modeltest 3.0 (Posada and Crandall, 1998), because of its dichotomous compari-

TABLE 3

Polymorphism in *Planipapillus* COI Sequences (473 sites)

Species	Individuals	Polymorphic sites
<i>P. biacinaces</i>	2	0
<i>P. cyclus</i>	2	0
<i>P. sp. 3</i> (Playground Road)	2	1 (T/C)
<i>P. sp. 7</i> (Bendoc)	2	0
<i>P. sp. 8</i> (Dinner Plain)	3	1 (A/G)

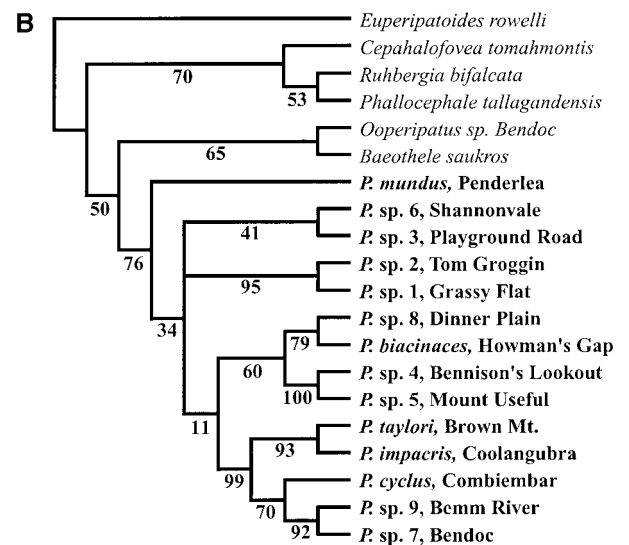
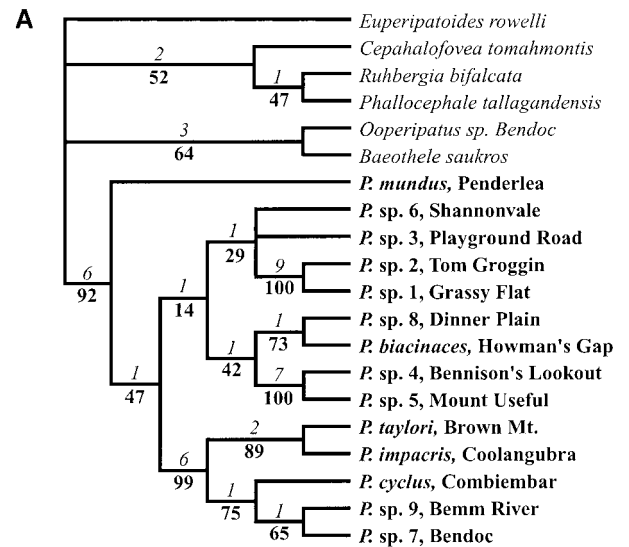


FIG. 4. Phylogenetic trees of COI sequences. (a) Strict consensus of four most parsimonious trees, showing decay support values above the branches and bootstrap percentages below. (b) Strict consensus of two most likely trees, showing bootstrap percentages.

son approach, selects the Tamura–Nei (TN) model (Tamura and Nei, 1993) rather than the K3ST, although K3ST gives a higher likelihood and the two models have the same number of parameters.

Two maximum-likelihood trees were identified, differing at a single node ($-\ln L = 2357.91230$; final parameter estimates: $\hat{\pi}_A = 0.33516$, $\hat{\pi}_C = 0.11490$, $\hat{\pi}_G = 0.13870$, $\hat{\alpha} = 0.58164$, $\hat{p}_{inv} = 0.53847$; estimated rate ratios among substitution types: A–C-type transversions = 1, A–T-type transversions = 3.25584, transitions = 10.21756). The ML trees, shown in Fig. 4b, differ from the MP trees at several deep ingroup nodes. However, according to the LSH test, none of the MP trees is significantly worse than the ML trees ($P > 0.82$) under the ML criterion, and according to the PSH

test, the ML trees are not significantly worse than the MP trees ($P > 0.76$) under the parsimony criterion. The trees agree on the recognition of two large clades, one including the five taxa from the eastern distribution (indeed, the relationships among these taxa are identical in all the optimal trees) and another involving a sister relationship between a *P. sp. 8* (Dinner Plain)–*P. biacinaces* clade and a *P. sp. 5* (Mt. Useful)–*P. sp. 4* (Bennison's Lookout) clade. The nodes that differ among the trees are weakly supported in each case. Interestingly, the best of the MP trees under ML with the K3STf+ Γ +I model is identical to the tree favored by ML under the JC model.

12S Sequences

The 12S sequences were aligned with gaps yielding a data set of 346 sites. The sequences included only two small regions of ambiguous alignment; 8 sites were excluded from subsequent analysis to accommodate these regions.

Among the ingroup taxa, 45 sites are variable and 19 MP informative. Uncorrected pairwise distances range from 0.003 to 0.076. The 20-sequence alignment includes 113 variable sites, 65 of them parsimony informative. These sequences are A+T biased (Table 2) but homogeneous in nucleotide composition ($P > 0.37$).

Parsimony analysis yields 38 shortest trees, each of 181 steps (CI on informative sites = 0.6772, RI = 0.7929). The strict consensus, shown in Fig. 5a with bootstrap and decay indices, is largely unresolved. The ingroup root is a polytomy, although the majority bootstrap tree roots the ingroup on the branch separating *P. mundus* from the remaining *Planipapillus*. Support for ingroup monophyly is strong, as is support for several clades including one comprising the *P. sp. 4* (Bennison's Lookout), *P. sp. 5* (Mount Useful), *P. sp. 8* (Dinner Plain), and *P. biacinaces* sequences.

Nested LRTs rejected the hypotheses of equal base frequencies, equal transition and transversion rates, equal rates among transition and transversion types, and equal rates among sites ($P < 0.005$ in each case), but did not reject the hypothesis of no invariable sites ($P = 0.41$). The GTR+ Γ model did not significantly improve fit over three-substitution-type models, of which K3STf+ Γ was the best (K3STf+ Γ vs GTR+ Γ ; $P = 0.77$).

Three ML trees were identified; these differ only in the placement of zero-length branches in the *P. cyclus*–*P. sp. 7* (Bendoc)–*P. taylori*–*P. impacris* clade. Figure 5b shows the ML tree with zero-length branches collapsed (–ln L = 1311.79053; final parameter estimates: $\hat{\pi}_A = 0.40768$, $\hat{\pi}_C = 0.05957$, $\hat{\pi}_G = 0.09749$, $\hat{\alpha} = 0.2964982$; estimated rate ratios: A–C-type transversions = 1, A–T-type transversions = 3.7074859, transitions = 13.9523293). The ML tree is identical to one of the MP trees but less resolved due to the trichotomy. The ML tree roots *Planipapillus* on the branch sepa-

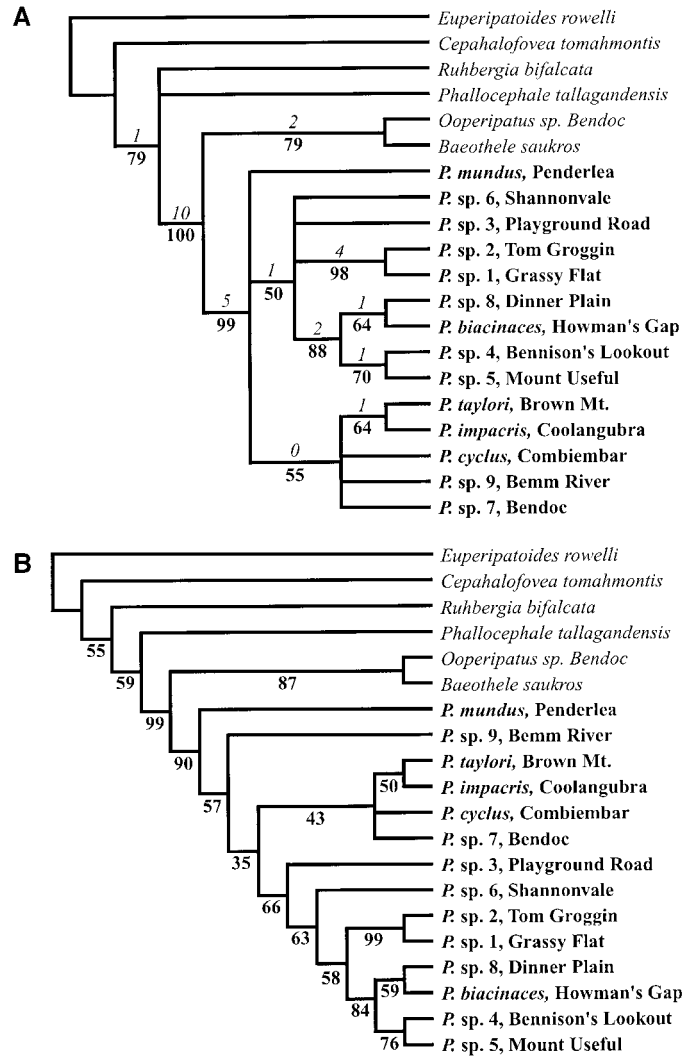


FIG. 5. Phylogenetic trees of 12S sequences. (a) Strict consensus of 38 most parsimonious trees, showing decay support values above the branches and bootstrap percentages below. (b) ML tree, showing bootstrap percentages.

rating *P. mundus* from the remaining taxa. It differs from the MP bootstrap tree primarily in the placement of the *P. sp. 9* (Bemm River) sequence; in the MP bootstrap tree, *P. sp. 9* (Bemm River) joins with the other taxa from the eastern edge of the *Planipapillus* range, whereas in the K3STf+ Γ ML tree it is more basal, sister to all *Planipapillus* but *P. mundus*. According to the LSH test, none of the 38 MP trees is significantly less likely than the ML tree ($P > 0.68$), and the ML tree, which requires only one extra step under the parsimony criterion, is not significantly worse than the MP trees according to the PSH test ($P > 0.87$). Because of the small amount of variation among the ingroup sequences, and the small amount of sequence data collected, the nodes which differ among the trees are likely to be the result of short branches and finite data.

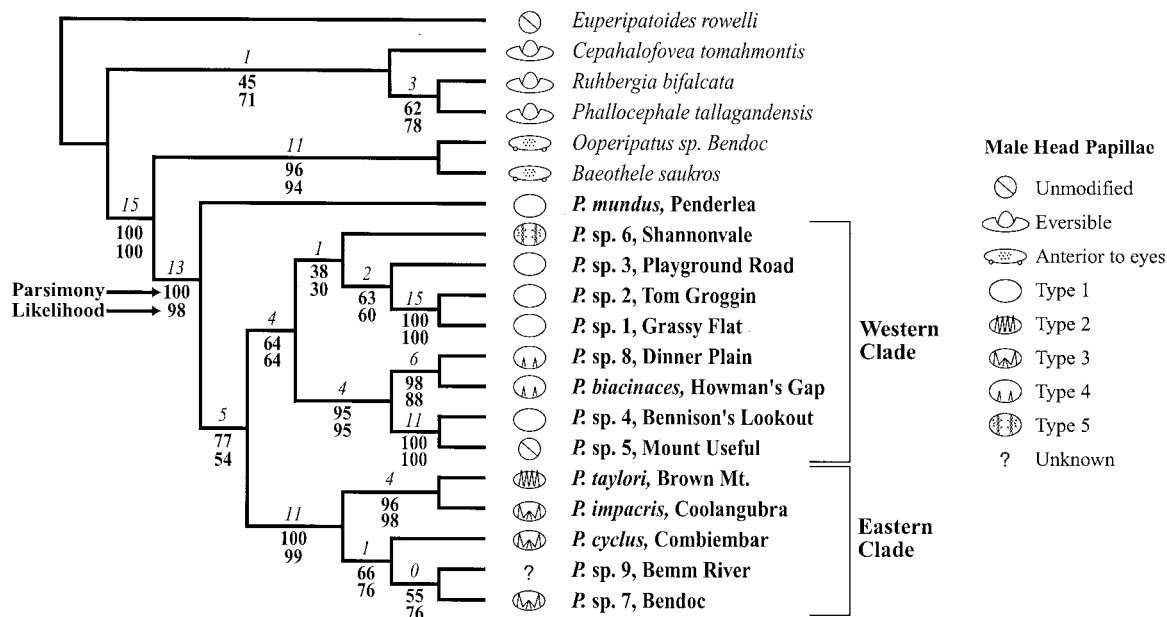


FIG. 6. Phylogenetic tree based on concatenated *ftz* intron, COI, and 12S sequences. This topology is one of two most parsimonious trees and is the most likely tree under both homogeneous and heterogeneous likelihood models. Parsimony decay support values are shown above the nodes. Parsimony bootstrap percentages are shown below the branches, and homogeneous likelihood bootstrap percentages below those. Male head papillae are indicated for each species; lawnhead symbols are shaded.

Combined-Data Phylogenetics

Homogeneity of the data sets cannot be rejected ($P = 0.62$) according to the partition homogeneity test (Farris *et al.*, 1995). The combined data set of 1161 characters includes 863 constant and 186 MP-informative characters, including the 9 *ftz* indel characters (among the ingroup taxa, 101 characters are MP informative). The two shortest trees, one of which is shown in Fig. 6, are 626 steps (CI on informative characters = 0.5740, RI = 0.6614). The two trees differ only in the placement of *P. sp. 9* (Bemm River), sister either to *P. cyclus* or *P. sp. 7* (Bendoc); as we lack information about the head structure of *P. sp. 9* (Bemm River), this ambiguity has no consequence for our interpretations of the evolution of these features. The sum of the lengths of the most parsimonious trees from the three sequences is 9 steps fewer than the total-evidence tree length, indicating that only 1.4% (9/626) of the tree length is due to incongruence among partitions. Seven of the 9 extra steps are from the fitting of the 12S data to the tree, and most of this incongruence involves relationships among the outgroups.

If the homogeneity of the partitions is accepted, the combined data set allows more confident estimation of relationships because of the greater data sampling. This logic is supported by the decay indices for many branches, which on the total-evidence tree are greater even than the sums of the decay indices for the same branches on the individual-sequence trees. For example, the clade of eight taxa from the western part of the

Planipapillus distribution is supported by 1 step in the COI tree, 1 step in the 12S tree, and no steps in the *ftz* tree, but by 4 steps in the total-evidence tree. Similarly, support for *P. mundus* as the sister to all other *Planipapillus* species jumps from 1 decay step to 5, and support for the clade of five eastern taxa jumps from 7 to 11.

The combined-data MP trees were compared to the ML trees favored by each of the partitions under the best ML models for those partitions, with the parameters estimated for the partition trees. The *ftz* data, analyzed under the F81 model, assigns the total-evidence MP trees the same likelihood as the tree identified as the *ftz* ML tree, which differs only in collapsing some zero-length branches. The COI data, under the K3STf+ Γ +I model, favors the COI ML trees over the total-evidence MP trees, but the MP trees are not significantly less likely (LSH test, $P > 0.78$). Similarly, the 12S data, under the K3STf+ Γ model, fails to reject the total-evidence MP trees (LSH test, $P > 0.50$).

Each of the partitions is compatible with the total-evidence MP trees under the parsimony criterion also. Notably, one of the two combined-data trees is identical to one of the COI MP trees, and the other is an insignificant one step longer for the COI data (PSH test, $P > 0.94$). The total-evidence trees require an extra seven steps for the 12S data, but they are not significantly less parsimonious than the 12S MP trees (PSH test, $P > 0.29$). The *ftz* data require 1 and 2 extra steps

to fit the two total-evidence MP trees, but in neither case is this significant (PSH test, $P > 0.63$).

The reciprocal test gives different results. Under parsimony, the combined data reject several of the partition trees, according to the PSH test. The 12S ML tree is significantly less parsimonious than the combined-data tree ($P < 0.05$), as is the *ftz* ML tree with zero-length branches collapsed ($P < 0.01$). The PSH test fails to reject other partition trees.

The combined data (1152 included sites) were also analyzed by ML, under the hypothesis that the process generating the sequences was homogeneous among the partitions. LRTs identified K3STf+ Γ +I as the best-fit model. A single maximum-likelihood tree, identical to one of the combined-data MP trees, was found ($-\ln L = 4509.21264$; final parameters: $\hat{\pi}_A = 0.35127$, $\hat{\pi}_C = 0.09581$, $\hat{\pi}_G = 0.12560$, $\hat{\alpha} = 0.67010$, $\hat{p}_{inv} = 0.57742$; estimated rate ratios: A–C-type transversions = 1, A–T-type transversions = 2.20269, transitions = 6.54649). The bootstrap support for the tree under this model is shown in Fig. 6. Interestingly, this tree is also the ML tree for the combined data under the JC model.

The combined-data ML tree is compatible with the individual partitions according to the LSH and PSH tests, as described above. The reciprocal test again gives different results. Under the ML criterion the combined data reject the *ftz* ML tree with zero-length branches collapsed (LSH test, $P < 0.01$), the 12S ML tree ($P < 0.05$), and 4 of the 38 12S MP trees ($P < 0.05$). The KH test (one-sided) rejects in addition 1 COI MP tree, all *ftz* MP trees, and 26 more of the 38 12S MP trees. These results illustrate that the SH test is not a trivial modification of the KH test.

The parameters estimated for the combined ML analysis are basically weighted averages of the parameters favored by each data partition, and so these average parameters do not fit any partition as well as the parameters estimated for that partition alone. We used LRTs to test whether likelihood is significantly improved by parameterizing each gene sequence separately, following Yang (1996). For each evaluated tree topology, model parameters and branch lengths are allowed to vary among the three sequence data sets. With the combined-data K3STf+ Γ +I tree as the test tree, this heterogeneous-partition model significantly improves likelihood (LRT statistic = 328.41484, $df = 83$ [including one rate-heterogeneity parameter; see Goldman and Whelan, 2000], $P < 10^{-6}$). Because of the complexity of the heterogeneous model, a thorough tree search is impossible. We evaluated the likelihood under the heterogeneous model of a population of candidate trees, specifically those that had been favored by any of the MP or ML analyses of the separate partitions. Parameter values were the final ML estimates for the separate analyses of each partition. Of the 60 candidate trees, the 1 favored by the homogeneous ML analysis (Fig. 6b) has the highest likelihood ($-\ln L =$

4345.00522). LSH tests with the heterogeneous model give the same results as the homogeneous model, rejecting the *ftz* ML, 12S ML, and 4 12S MP trees.

DISCUSSION

Our favored hypothesis (Fig. 6) of phylogenetic relationships among *Planipapillus* species is one of two optimal trees under the maximum-parsimony criterion and the sole optimal tree under the maximum-likelihood criterion with models ranging from the one-parameter JC model to the homogeneous K3STf+ Γ +I to the heterogeneous-partition model. We consider first the implications of our results for phylogenetic methods and then address the implications of the phylogeny for interpretations of morphological evolution and biogeographic history in *Planipapillus*.

Phylogenetic Methods

In the present analysis, a nonstandard, three-substitution-type model was favored for two data sets and for the homogeneous analysis of the concatenated data set. The K3STf model, which incorporates unequal base frequencies to accommodate A+T bias and then allows different rates for transversions that change A+T% and those that conserve it, is clearly appropriate for A+T/G+C-biased sequences yet has not been widely used. We believe that its identification as the best-fit model for two mitochondrial sequences recommends its use more generally. Likelihood ratio tests have become the standard approach to identifying the best-fit model for maximum-likelihood approaches to phylogenetics (Huelsenbeck and Crandall, 1997; Cunningham *et al.*, 1998). In many implementations of these tests, however, only the popular two- and six-substitution-type models are considered. Rejection of the two-parameter model (HKY85) results in adoption of the six-parameter GTR model, without consideration of the fit of intermediate models. We suspect that for data sets of the modest size most commonly studied, GTR models will often be fitting noise. If this is the case, consideration of three-substitution-type models, including K3STf and TN, may reduce the number of nuisance parameters to be estimated, resulting in lower-variance estimates of branch lengths and improved phylogenetic accuracy (Cunningham *et al.*, 1998). In its newest implementation (Version 3.0), Modeltest (Posada and Crandall, 1998) includes three-substitution-type models. However, because it compares models according to a predefined dichotomous program, Modeltest can miss a best-fit model if models with the same number of parameters are on different paths in the dichotomy. For our COI data set, Modeltest favors the TN model, whereas the K3STf model, with the same number of parameters, confers a higher likelihood on the test tree.

We used Shimodaira–Hasegawa tests to show that

the combined-data trees are also supported by each gene individually. Given a small amount of data from a single sequence, the maximum-parsimony and maximum-likelihood function surfaces are relatively flat and many topologies are within the confidence interval. For this reason, it is valuable to combine all the data and try to increase the amount of resolving power, i.e., by steepening the surfaces. That seems to have worked in the present case, as the combined data reject several of the trees based on the separate partitions. Moreover, all methods ultimately support the same tree, and both bootstrap and support index values increase when the data are combined. Note, however, that the Shimodaira–Hasegawa tests prove considerably more conservative than the inappropriate *a posteriori* applications of the Kishino–Hasegawa test; applications of the KH test in the literature must be treated cautiously (Goldman *et al.*, 2000).

Although the 12S data fit the favored total-evidence tree less well than the other partitions, it is evident that the incongruence is concentrated in relationships among the outgroups. A reasonable inference is that the 12S alignment among the outgroups is incorrect and implies inaccurate positional homologies, an illustration of the importance of dense taxon sampling to sequence alignment. Loops in rRNAs grow and shrink by insertions and deletions, but the range of possible lengths is constrained. As a result, more distantly related sequences may by chance have the same lengths, despite the occurrence of insertions and deletions on the intervening branches. This presents little danger for our closely related ingroup sequences, but may be responsible for the incongruence among the outgroups. Because the ingroup alignment appears unambiguous, outgroup incongruence should have little effect on the inferred ingroup relationships.

Planipapillus Phylogeny and Evolution

In our favored phylogeny (Fig. 6), *Ooperipatus* and *Baeothele*, oviparous taxa with modified male head papillae anterior to the eyes, are the closest outgroups to *Planipapillus*. Ovoviviparous species with eversible head structures are more distantly related. Within *Planipapillus*, *P. mundus* is the sister to the clade containing all other species. The latter is divided into two clades, one including taxa from the western part of the Australian Alps, and another comprising eastern *Planipapillus* taxa. In the western clade, most relationships are very well supported, excepting the position of *P. sp. 6* (Shannonvale). This taxon appears to have branched from the *P. sp. 3* (Playground Road)–*P. sp. 2* (Tom Groggin)–*P. sp. 1* (Grassy Flat) lineage soon after these lineages split from the remaining Alpine taxa. In the western clade, the initial split was between a northern clade, including *P. taylori* and *P. impacris*, and a southern clade, with *P. cyclus*, *P. sp. 7* (Bendoc),

and *P. sp. 9* (Bemm River). One interesting result is that divergences are well supported at several levels of the phylogeny; splits are not all early or late, but spread throughout the phylogeny.

Reid (1996) included four *Planipapillus* species in her study, three of which were considered here. Based primarily on color patterns, the distribution of the cranial papillae, and features of the head structures, Reid concluded that *P. taylori* is basal within *Planipapillus* and *P. biacinaces* and *P. mundus* are derived. This result is incompatible with our phylogeny, which has *P. mundus* as basal. More recently, Reid (2000), in an analysis including many more *Planipapillus* species, concluded that morphological characters could not resolve relationships within the clade. Moreover, she notes that many of the characters differentiating the species are part of the male head structure and may not represent independent characters. Ultimately, we anticipate that complete morphological characterizations of the undescribed *Planipapillus* species, and an analysis incorporating both morphological and nucleotide sequence data, will test the phylogenetic hypothesis forwarded here.

The very strongly supported position of *Ooperipatus* and *Baeothele* as the closest outgroup to *Planipapillus*, with *Cephalofovea*, *Phallocephale*, and *Ruhbergia* more distantly related, has implications for both the evolution of reproductive mode and the homologies of *Planipapillus* head structures. Unresolved in the study of Reid (1996), these relationships indicate that oviparity is shared among *Planipapillus* and its close relatives and need not have arisen independently in each of these lineages. Whether oviparity is ancestral in Australian onychophorans or derived in the common ancestor of *Planipapillus* and the other oviparous taxa cannot be answered by our data (see, e.g., Lee and Shine (1998) for the difficulty of such inferences).

Reid (1996) coded the *Planipapillus* head structure as unrelated to head structures consisting of modified papillae (e.g., *Ooperipatus* and *Baeothele*) or eversible organs anterior of the eyes (e.g., *Phallocephale*, *Cephalofovea*, and *Ruhbergia*). Because both proximal outgroups to *Planipapillus* have modified head structures, our phylogeny suggests that the sexually dimorphic head structures of *Planipapillus* may be related to the head structures of other onychophorans, contrary to Reid (1996). The nearest outgroup, the clade of *Ooperipatus* and *Baeothele*, has sexually dimorphic head papillae anterior to the eyes. The next outgroup includes species with eversible male head structures anterior to the eyes. Parsimony inference thus implies that either an ancestor of *Planipapillus* possessed modified male head papillae anterior to the eyes or that the modified papillae in the *Ooperipatus*–*Baeothele* clade and the eversible-structure clade evolved separately.

In the first case, the ancestor of *Planipapillus* had modified male head papillae anterior to the eyes which

then migrated to a more posterior position or these papillae were lost in the ancestor and modified head papillae posterior to the eyes were acquired separately. Since *Planipapillus* shares with the eversible-structure clade use of the head structure for spermatophore transfer (Reid, 2000; Tait and Norman, 2001), it is parsimonious to infer that the head structures are homologous. Thus, the modified male head papillae of *Ooperipatus* and *Baeothele* may be derived from spermatophore transfer structures, although their morphology appears to preclude such a function currently.

The second possible parsimony inference, that the modified papillae anterior to the eyes evolved separately in the *Ooperipatus*-*Baeothele* clade and the eversible-head-structure clade, implies that the *Planipapillus* head papillae are not homologous to other head structures. In this case, the presence of modified head papillae is convergent among *Planipapillus*, the eversible-head-structure clade, and the *Ooperipatus*-*Baeothele* clade; further, the use of modified male head papillae for spermatophore transfer emerges as a convergence between the eversible-structure clade and *Planipapillus*. We consider the first scenario, that *Planipapillus* is derived from an ancestor with modified papillae anterior to the eyes, more plausible, as it implies that the two features unique among onychophorans, the modified male head papillae and their use in spermatophore transfer, represent homologies. This model raises questions about the coevolution of the male head structures and female reproductive structures and about the mating behavior of *Ooperipatus* and *Baeothele*, which we infer to be descended from a head-mating ancestor.

Within *Planipapillus*, a parsimonious reading of the phylogeny suggests that the plain lawn-head is ancestral and that spikes within the lawn evolved independently in three lineages. The two-spiked head (class 4) evolved in the common ancestor of *P. biacinaces* and *P. sp. 8* (Dinner Plain), the four-spiked head (classes 2 and 3) arose in the ancestor of the eastern *Planipapillus* clade, and the class 5 head, with its rows of small spikes, arose in the lineage leading to *P. sp. 6* (Shannonvale). Within the eastern clade, the class 3 head structure with two small incurved spikes and two outer straight spikes gave rise to the class 2 structure, four straight, equal-length spikes, found only in *P. taylori*. Although we have not observed the head structure from *P. sp. 9* (Bemm River), we predict from the phylogeny that it will have class 3 modified head papillae.

Independent origins of spikes in three lineages within *Planipapillus*, plus additional origins of spikes within the eversible-structure clade, suggest that the head spikes may be serving an adaptive function. Reid (2000) described mating behavior in *P. annae*, which has class 1 head papillae, with no spikes. She observed the papillae surrounding the bare patch clasping the female's ovipositor while the coupled animals walked

around. In most *Planipapillus* species these surrounding papillae are enlarged and bear sensory bristles (Fig. 2; Reid, 2000). Reid's (2000) observations suggest that the surrounding papillae may play a role not only in chemo- and mechanoreception, but in the physical maintenance of the coupling. Spikes may be further elaborations to maintain coupling. Alternatively, the spikes may function to hold the spermatophore in place. The morphological and behavioral relationships among the male head structure, spermatophore, and female reproductive structures warrant further study.

The discovery of *P. sp. 5* (Mt. Useful), which lacks modified head papillae, poses additional questions. Parsimony unequivocally reconstructs a class I head structure for its ancestor. An adaptive explanation for the three origins of spikes must take into account the opposite situation, the loss of modified head papillae in *P. sp. 5* (Mt. Useful).

Many features of onychophoran biology remain enigmatic, but the recently discovered diversity of Australian Onychophora creates an opportunity to investigate diversification in morphological and molecular characteristics in many clades in parallel. Our study of *Planipapillus* represents a first effort to establish a framework for addressing these issues.

ACKNOWLEDGMENTS

We are grateful to Stuart Dennis, Kathy Tsang, and Don Bromhead for help in the field, to Ginny Sargent and Alex Wilson for help in the lab, to Sue Doyle for SEM, and to Ross Parks for map and plate preparation. Paul Sunnucks, Ehab Abouheif, and Jim Balhoff provided helpful comments on a draft. This work was supported by a Fulbright Fellowship and NSF predoctoral fellowship to M.V.R. and ARC funding to D.M.R.

REFERENCES

- Bremer, K. (1988). The limits of amino acid sequence data in angiosperm phylogenetic reconstruction. *Evolution* **42**: 795–803.
- Briscoe, D. A., and Tait, N. N. (1995). Allozyme evidence for extensive and ancient radiations in Australian Onychophora. *Zool. J. Linn. Soc.* **114**: 91–102.
- Buckley, T. R., Simon, C., Shimodaira, H., and Chambers, G. K. (2001). Evaluating hypotheses on the origin and evolution of the New Zealand alpine cicadas (*Maoricicada*) using multiple comparison tests of tree topology. *Mol. Biol. Evol.* **18**: 223–234.
- Cunningham, C. W., Zhu, H., and Hillis, D. M. (1998). Best-fit maximum-likelihood models for phylogenetic inference: Empirical tests with known phylogenies. *Evolution* **52**: 978–987.
- Farris, J. S., Källersjö, M., Kluge, A. G., and Bult, C. (1995). Testing significance of incongruence. *Cladistics* **10**: 315–319.
- Felsenstein, J. (1981). Evolutionary trees from DNA sequences: A maximum likelihood approach. *J. Mol. Evol.* **17**: 368–376.
- Felsenstein, J. (1985). Confidence limits on phylogenies: An approach using the bootstrap. *Evolution* **39**: 783–791.
- Felsenstein, J. (2000). "PHYLP: Phylogeny Inference Package," version 3.573c, distributed by the author, University of Washington, Seattle.
- Ghiselin, M. T. (1984). *Peripatus* as a living fossil. In "Living Fossils"

- (N. Eldredge and S. M. Stanley, Eds.), pp. 214–217. Springer-Verlag, New York.
- Gleeson, D. M., Rowell, D. M., Tait, N. N., Briscoe, D. A., and Higgins, A. V. (1998). Phylogenetic relationships among Onychophora from Australasia inferred from the mitochondrial cytochrome oxidase subunit I gene. *Mol. Phylogenet. Evol.* **10**: 237–248.
- Goldman, N. (1993). Statistical tests of models of DNA substitution. *J. Mol. Evol.* **36**: 182–198.
- Goldman, N., and Whelan, S. (2000). Statistical tests of gamma-distributed rate heterogeneity in models of sequence evolution in phylogenetics. *Mol. Biol. Evol.* **17**: 975–978.
- Goldman, N., Anderson, J. P., and Rodrigo, A. G. (2000). Likelihood-based tests of topologies in phylogenetics. *Syst. Biol.* **49**: 652–670.
- Grenier, J. K., Garber, T. L., Warren, R., Whittington, P. M., and Carroll, S. (1997). Evolution of the entire arthropod Hox gene set predated the origin and radiation of the onychophoran/arthropod clade. *Curr. Biol.* **7**: 547–553.
- Heyler, D., and Poplin, C. M. (1988). The fossils of Montceau-les-Mines. *Sci. Am.* **259**: 70–76.
- Huelsenbeck, J. P., and Crandall, K. A. (1997). Phylogeny estimation and hypothesis testing using maximum likelihood. *Annu. Rev. Ecol. Syst.* **28**: 437–466.
- Jukes, T. H., and Cantor, C. R. (1969). Evolution of protein molecules. In "Mammalian Protein Metabolism" (H. N. Munro, Ed.), pp. 21–132. Academic Press, New York.
- Kimura, M. (1981). Estimation of evolutionary distances between homologous nucleotide sequences. *Proc. Natl. Acad. Sci. USA* **78**: 454–458.
- Kishino, H., and Hasegawa, M. (1989). Evaluation of the maximum likelihood estimate of the evolutionary tree topologies from DNA sequence data, and the branching order in Hominoidea. *J. Mol. Evol.* **29**: 170–179.
- Lee, M. S. Y., and Shine, R. (1998). Reptilian viviparity and Dollo's law. *Evolution* **52**: 1441–1450.
- Lincoln, S. E., Daly, M. J., and Lander, E. S. (1991). Primer: A computer program for automatically selecting per primers. (Version 0.5). Whitehead Institute for Biomedical Research, Cambridge, MA.
- New, T. R. (1995). Onychophora in invertebrate conservation: Priorities, practices and prospects. *Zool. J. Linn. Soc.* **114**: 77–89.
- Posada, D., and Crandall, K. A. (1998). Modeltest: Testing the model of DNA substitution. *Bioinformatics* **14**: 817–818.
- Ramskold, L., and Junyuan, C. (1998) Cambrian lobopodians: Morphology and phylogeny. In "Arthropod Fossils and Phylogeny" (G. Edgecombe, Ed.), pp. 107–150. Columbia Univ. Press, New York.
- Reid, A. L. (1996). Review of the Peripatopsidae (Onychophora) in Australia, with comments on Peripatopsid relationships. *Invertebr. Taxon.* **10**: 663–936.
- Reid, A. L. (2000). Eight new *Planipapillus* (Onychophora: Peripatopsidae) from southeastern Australia. *Proc. Linn. Soc. NSW* **122**: 1–32.
- Reid, A. L., Tait, N. N., and Briscoe, D. A. (1995). Morphological, cytogenetic and allozymic variation within *Cephalofovea* (Onychophora: Peripatopsidae) with descriptions of three new species. *Zool. J. Linn. Soc.* **114**: 115–138.
- Rowell, D. M., Higgins, A. V., Briscoe, D. A., and Tait, N. N. (1995). The use of chromosomal data in the systematics of viviparous onychophorans from Australia (Onychophora: Peripatopsidae). *Zool. J. Linn. Soc.* **114**: 139–153.
- Rowell, D. M., Rockman, M. V., and Tait, N. N. (in press).
- Shimodaira H., and Hasegawa, M. (1999). Multiple comparisons of log-likelihoods with applications to phylogenetic inference. *Mol. Biol. Evol.* **16**: 1114–1116.
- Shiozawa, D. K., Kudo, J., Evans, R. P., Woodward, S. R., and Williams, R. N. (1992). DNA extraction from preserved trout tissues. *Great Basin Nat.* **52**: 29–34.
- Simon, C., Frati, F., Beckenbach, A., Crespi, B., Liu, H., and Flook, P. (1994). Evolution, weighting, and phylogenetic utility of mitochondrial gene-sequences and a compilation of conserved polymerase chain-reaction primers. *Ann. Entomol. Soc. Am.* **13**: 651–701.
- Sunnucks, P., and Wilson, A. C. C. (1999). Microsatellite markers for the onychophoran *Euperipatoides rowelli*. *Mol. Ecol.* **8**: 899–900.
- Sunnucks, P., Curach, N., Young, A., French, J., Cameron, R., Briscoe, D. A., and Tait, N. N. (2000a). Reproductive biology of the onychophoran *Euperipatoides rowelli*. *J. Zool.* **250**: 447–460.
- Sunnucks, P., Wilson, A. C. C., Beheregaray, L. B., French, J., Zenger, K., and Taylor, A. C. (2000b). SSCP is not so difficult: The application and utility of single-stranded conformation polymorphism in evolutionary biology and molecular ecology. *Mol. Ecol.* **9**: 1699–1710.
- Swofford, D. L. (1998). "PAUP*. Phylogenetic analysis using parsimony (* and other methods). (Version 4). Sinauer, Sunderland, MA.
- Tait, N. N., and Briscoe, D. A. (1990). Sexual head structures in the Onychophora: Unique modifications for sperm transfer. *J. Nat. Hist.* **24**: 1517–1527.
- Tait, N. N., and Briscoe, D. A. (1995). Genetic differentiation within New Zealand Onychophora and their relationships to the Australian fauna. *Zool. J. Linn. Soc.* **114**: 103–113.
- Tait, N. N., and Norman, J. M. (2001). Novel mating behaviour in *Florellicept stutchburyae* n. gen., n. sp. (Onychophora: Peripatopsidae) from Australia. *J. Zool.* **253**: 301–308.
- Tait, N. N., Briscoe, D. A., and Rowell, D. M. (1995) Onychophora—Ancient and modern radiations. *Mem. Assoc. Australas. Paleontol.* **18**: 21–30.
- Tamura, K., and Nei, M. (1993). Estimation of the number of nucleotide substitutions in the control region of mitochondrial DNA in humans and chimpanzees. *Mol. Biol. Evol.* **10**: 512–526.
- Thompson, I., and Jones, D. S. (1980). A possible onychophoran from the Middle Pennsylvanian Mazon Creek beds of northern Illinois. *J. Paleontol.* **54**: 588–596.
- Thompson, J. D., Gibson, T. J., Plewniak, F., Jeanmougin, F., and Higgins, D. G. (1997). The ClustalX windows interface: Flexible strategies for multiple sequence alignment aided by quality analysis tools. *Nucleic Acids Res.* **24**: 4876–4882.
- Trewick, S. A. (1998). Sympatric cryptic species in New Zealand Onychophora. *Biol. J. Linn. Soc.* **63**: 307–329.
- Trewick, S. A. (1999). Molecular diversity of Dunedin peripatus (Onychophora: Peripatopsidae). *N.Z.J. Zool.* **26**: 381–391.
- Trewick, S. A. (2000). Mitochondrial DNA sequences support allozyme evidence for cryptic radiation of New Zealand Peripatoides (Onychophora). *Mol. Ecol.* **9**: 269–281.
- Yang, Z. (1996). Maximum-likelihood models for combined analysis of multiple sequence data. *J. Mol. Evol.* **42**: 587–596.
- Yang, Z. (2000). Phylogenetic analysis by maximum likelihood (PAML). (Version 3.0). University College, London.
- Yang, Z., Goldman, N., and Friday, A. (1995). Maximum likelihood trees from DNA sequences: A peculiar statistical estimation problem. *Syst. Biol.* **44**: 384–399.